DOI: 10.7641/CTA.2015.14137

带有饱和的电机伺服系统非奇异终端滑模funnel控制

陈 强†, 汤筱晴

(浙江工业大学 信息工程学院, 浙江 杭州 310023)

摘要: 本文提出一种非奇异终端滑模funnel控制(NTSMFC)方法, 实现带有饱和输入电机伺服系统的指定性能跟踪控制. 根据中值定理, 非光滑饱和函数转化为放射形式, 并且应用一个简单的神经网络进行逼近和补偿. 为保证跟踪误差被限制在指定的界限内, 同时为避免构建复杂的barrier李雅普诺夫函数或逆函数, 本文采用一个新的限制变量. 然后, 构建非奇异终端滑模funnel控制器保证电机伺服系统的指定跟踪性能. 该方法无需事先已知输入饱和函数的界限等先验知识, 且基于李雅普诺夫函数设计可以保证位置跟踪误差的收敛性, 最后给出仿真对比实例证明了该方法的有效性.

关键词: funnel控制; 非奇异终端滑模; 神经网络; 输入饱和

中图分类号: TP273 **文献标识码**: A

Nonsingular terminal sliding-mode funnel control for prescribed performance of motor servo systems with unknown input saturation

CHEN Qiang†, TANG Xiao-qing

(College of Information Engineering, Zhejiang University of Technology, Hangzhou Zhejiang 310023, China)

Abstract: A nonsingular terminal sliding-mode funnel control (NTSMFC) scheme is proposed for tracking the prescribed performance of motor servo systems with unknown input saturation. Based on the mean-value theorem, the non-smooth saturation is transformed into a smooth affine function, and then is approximated and compensated by using a simple sigmoid neural network. Rather than constructing the complex barrier Lyapunov function or inversely transformed function, we employed a new constraint variable to force the tracking error to fall into prescribe boundaries. Then, a nonsingular terminal sliding-mode funnel control is developed for tracking the prescribed performance of the motor servo system. With the proposed scheme, no prior knowledge is required on the bound of input saturation, and the convergence of the position tracking error is guaranteed via the Lyapunov synthesis. Comparison simulation examples are given to illustrate the effectiveness of the proposed method.

Key words: funnel control; nonsingular terminal sliding mode control; neural network; input saturation

1 Introduction

Over the past decades, motor servo systems have been widely studied in motion control applications[1–3]. The mechanical connection between servo motors and mechanical devices produces non-smooth nonlinear constraints on their outputs and/or inputs in the form of the physical stoppage, saturation, hysteresis, and dead-zone. During operation, violation of the constraints leads to performance degradation, hazards or system damage. For the output constraint, there are some effective methods for position, velocity, and force constraints existing in motor servo systems. By using the logarithmic function in the Lyapunov function design, a barrier Lyapunov function (BLF) is constructed, in which a symmetric or asymmetric constraint is utilized to constrain the state variable of the control system, so that the tracking errors can be indirectly constrained[4–6]. However, the expression of BLF is complex, and extra efforts are needed to ensure the continuity and differentiability. In [7–9], a prescribed performance control (PPC) scheme is proposed, and the tracking error of a nonlinear system is transformed into a new error by constructing the inverse of the transformation function. Therefore, the prescribed tracking performance of the transient property and the steady-state error can be guaranteed. But PPC scheme may cause a singularity problem since the inverse transformation function includes a partial differential terms.

Being a non-model-based (memory less) constraint technique, the funnel control is proposed to guarantee the prescribed transient behavior and asymptotic tracking of the system[10–13]. This technique bypasses the difficulties of identification and estimation of traditional high-gain adaptive control. Recently, a new error-constraint variable is designed as a virtual control variable in the backstep-

Received 14 October 2014; accepted 29 May 2015.

†Corresponding author. E-mail: sdnjchq@zjut.edu.cn; Tel.: +86 571-85290531.

Supported by National Natural Science Foundation of China (61403343), Scientific Research Foundation of the Education Department of Zhejiang Province, China (Y201329260) and Natural Science Foundation of Zhejiang University of Technology (1301103053408).

ping design to ensure the prescribed transient and steady-state performance[14], and thus the aforementioned complex transformation function is not needed any more. In [15], a funnel dynamic surface control with prescribed performance is proposed to overcome the explosion of complexity problem in the backstepping technique, and the tracking performance of closed-loop system is guaranteed.

Sliding mode control (SMC) is one of the most useful approaches to deal with system uncertainties and bounded disturbances, and has been widely applied in various fields[16–17]. The traditional linear sliding mode control scheme can guarantee the asymptotical convergence of tracking errors when time goes to the infinity. Recently, many research works have focused on the finite-time convergence of tracking errors. Man and Yu[18] proposed a terminal sliding mode control (TSMC) scheme by introducing a nonlinear term in the SMC design and the tracking error can be guaranteed to converge within a finite time. However, there are two disadvantages of TSMC, i.e., the singularity problem and requirement of the uncertainty bound. To overcome the singularity problem, Feng, et al.[19] and Yu, et al.[20] proposed nonsingular terminal sliding mode control (NTSMC) methods. Besides, Chen, et al[21] utilized a recurrent Hermite neural network (RHNN) to estimate the lumped uncertainty online when designing the nonsingular terminal sliding surface, and hence the lumped uncertainty bound is unnecessary.

As one of the most important non-smooth nonlinearities, saturation on hardware dictates that the magnitude of the control signal is always constrained, which often severely limits system performance, giving rise to undesirable inaccuracy or leading instability[22]. So far, many significant results on the control design for the systems with input saturation have been obtained[23–27]. However, the lower and upper limits of the saturation constraints should be exactly known or estimated for controllers design. Recently, several research work has been investigated without using the prior knowledge of saturation bounds. Wen et al.[28] uses a smooth non-affine function of the control input signal to approximate the non-smooth saturation function, and a Nussbaum function is introduced to compensate for the nonlinear term arising from the input saturation. Based on the idea of [28], Wang et al.[29] transforms the non-affine function of the system into an affine form, and an adaptive control scheme is derived without requiring the prior knowledge of input saturation bounds.

In this paper, we propose a nonsingular terminal sliding mode funnel control to achieve a prescribed tracking performance for motor servo systems with unknown input saturation. A smooth and affine function is used to solve the input saturation problem. Meanwhile, to avoid using the complex barrier Lyapunov function or inverse transformed function, a funnel constraint variable is utilized in constructing the nonsingular terminal sliding mode scheme to force the tracking error fall within prescribe boundaries. No prior knowledge of the input saturation bounds is required in the proposed method, and the effectiveness is demonstrated by simulation results.

2 Problem formulation and preliminaries

2.1 System description

The mechanical dynamics of the motor servo system can be described as follows:

$$\begin{cases} m\ddot{x} + f(\boldsymbol{x}, t) + d(\boldsymbol{x}, t) = k_0 v(u), \\ y = x(t), \end{cases} \tag{1}$$

where $\boldsymbol{x} = [x,\ \dot{x}]^{\mathrm{T}} \in \mathbb{R}^2$, $u(t) \in \mathbb{R}$, $y \in \mathbb{R}$ are state variables, the control input voltage to the motor and the output from the motor, respectively; x is the position, m is the inertia, k_0 is a positive control gain (the force constant), $f(\boldsymbol{x}, t)$ is the friction force; $d(\boldsymbol{x}, t)$ represents a bounded disturbance modeling nonlinear elastic forces generated by coupling and protective covers, measurement noise, power electronics disturbances and other uncertainties. $v(u) \in \mathbb{R}$ is the plant input subject to saturation nonlinearity described by

$$v(u) = \mathrm{sat}(u) = \begin{cases} v_{\max} \mathrm{sgn}\, u, & |u| \geqslant v_{\max}, \\ u, & |u| < v_{\max}, \end{cases} \tag{2}$$

where $v_{\max}$ is an unknown parameter of input saturation.

For convenience of the controller design, defining $x_1 = x$, $x_2 = \dot{x}$, the mechanical dynamics of the motor servo system can be transformed into

$$\begin{cases} \dot{x}_1 = x_2, \\ \dot{x}_2 = -\dfrac{f(\boldsymbol{x}, t) + d(\boldsymbol{x}, t)}{m} + \dfrac{k_0}{m} v(u), \\ y = x_1. \end{cases} \tag{3}$$

Without loss of generality, two technical assumptions are made to pose the problem in a tractable manner.

1) The desired position trajectory y_{d}, the time derivative $\dot{y}_{\mathrm{d}}$ and $\ddot{y}_{\mathrm{d}}$ are both bounded and smooth signals.

2) The angular position and velocity, x_1 and x_2, are measurable.

2.2 Nonlinear saturation model

Clearly, the relationship between the applied control $v(t)$ and the control input $u(t)$ has a sharp corner when $|u(t)| = v_{\max}$. As shown in Fig.1, the saturation is approximated by a smooth non-affine function defined as

$$g(u) = v_{\max} \times \tanh(\frac{u}{v_{\max}}) = v_{\max} \times \frac{\mathrm{e}^{u/v_{\max}} - \mathrm{e}^{u/v_{\max}}}{\mathrm{e}^{u/v_{\max}} + \mathrm{e}^{u/v_{\max}}}. \tag{4}$$

Then, $v = \mathrm{sat}(u)$ in (2) can be expressed in the following form

$$v = \mathrm{sat}(u) = g(u) + d_1(u), \tag{5}$$

where $d_1(u) = \mathrm{sat}(u) - g(u)$ is a bounded function and its bound can be obtained as

$$|d_1(u)| = |\mathrm{sat}(u) - g(u)| \leqslant v_{\max}(1 - \tanh(1)) = D,$$

where D is the upper bound of $|d_1(u)|$.

According to the mean-value theorem[29], there exists a constant ξ with $0 < \xi < 1$,such that

$$g(u) = g(u_0) + g_{u_\xi}(u - u_0), \tag{6}$$

where $g_{u_\xi} = \dfrac{\partial g(u)}{\partial u}|_{u=u_\xi}$, $u_\xi = \xi u + (1-\xi)u_0$ and $u_0 \in [0, u]$. By choosing $u_0 = 0$, (6) can be rewritten in the following affine form

$$g(u) = g_{u_\xi} u. \tag{7}$$

Substituting (7) and (5) into (3), we can obtain

$$\begin{cases} \dot{x}_1 = x_2, \\ \dot{x}_2 = h(\boldsymbol{x}, t) + bu, \\ y = x_1, \end{cases} \tag{8}$$

where $h(\boldsymbol{x}, t) = -\dfrac{f(\boldsymbol{x}, t) + d(\boldsymbol{x}, t)}{m} + d_1$, $b = \dfrac{k_0 g_{u_\xi}}{m}$.

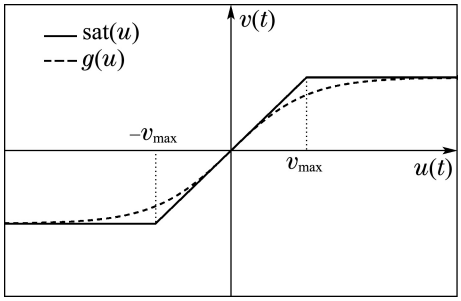

Fig. 1 Saturation $\mathrm{sat}(u)$ and smooth function $g(u)$

2.3 Neural network approximation

Due to good capabilities in function approximation, neural networks (NNs) are usually used for the approximation of nonlinear functions. The following neural network with a simple structure and a fast convergence property will be used to approximate the continuous function

$$h(\boldsymbol{X}) = W^{*\mathrm{T}}\phi(\boldsymbol{X}) + \varepsilon, \tag{9}$$

where $W^* \in \mathbb{R}^{n_1 \times n_2}$ is the ideal weight matrix, $\phi(\boldsymbol{X}) \in \mathbb{R}^{n_1 \times 1}$ is the basis function of the neural network, ε is the neural network approximation error satisfying $|\varepsilon| \leqslant \varepsilon_N$, $\phi(\boldsymbol{X})$ can be chosen as the commonly used sigmoid function, which is in the following form

$$\phi(\boldsymbol{X}) = \frac{a}{b + \mathrm{e}^{(-\boldsymbol{X}/c)}} + d \tag{10}$$

with a, b, c and d being appropriate parameters.

Remark 1 The employed neural network with sigmoid function represents a class of linearly parameterized approximation methods, and can be replaced by any other approximation approaches such as spline functions, RBF functions or fuzzy systems. However, the structure of the employed neural network in the this paper is simpler than the other neural networks that are commonly used in other works. There is no hidden layer in the employed NN, in which five inputs and one output are included and the corresponding weight matrix is 5×1.

3 Nonsingular terminal sliding mode funnel control

3.1 Funnel error variable

Funnel control is a strategy that employs a time-varying gain $\rho(t)$ to control systems of class S with a relative degree $r = 1$ or 2, stable zero dynamics, and known high-frequency gains. The system S is governed by the funnel controller with the control input

$$u(t) = \rho(F_\phi(t), \psi(t), \|e(t)\|) \times e(t), \tag{11}$$

where $e(t) = y_1 - y_\mathrm{d}$ is the tracking error, $\rho(\cdot)$ denotes the control gain.

As shown in Fig.2, evaluate the vertical distance at the actual time between the funnel boundary $F_\phi(t)$ and the Euclidian error norm $\|e(t)\|$ as

$$d_\mathrm{v}(t) = F_\phi(t) - \|e(t)\|.$$

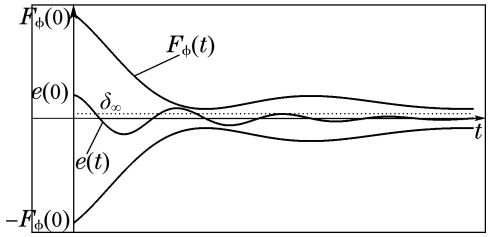

Fig. 2 Basic concept of the funnel control

The funnel boundary is given by the reciprocal of an arbitrarily chosen bounded, continuous and positive function $\varphi(t) > 0$ for all $t \geqslant 0$ with $\sup\limits_{t \geqslant 0} \varphi(t) < \infty$. The funnel is defined as

$$F_\phi(t) \to \{e \in \mathbb{R}^m | \varphi(t) \times \|e(t)\|\}.$$

To ensure that the error $e(t)$ evolves inside the funnel $F_\phi(t)$, the expression of $\rho(\cdot)$ can be chosen as

$$\rho(t) = \frac{1}{F_\phi(t) - \|e(t)\|}. \tag{12}$$

From (12) we can see that, when the gain $\rho(t)$ increases, the error $e(t)$ approaches the boundary F_ϕ, and when the gain $\rho(t)$ decreases conversely, the error $e(t)$ becomes small. A proper funnel boundary to prescribe the performance is selected as

$$F_\phi(t) = \delta_0 \mathrm{e}^{-a_0 t} + \delta_\infty, \tag{13}$$

where $\delta_0 \geqslant \delta_\infty > 0$, $\delta_\infty = \lim\limits_{t \to \infty} \inf F_\phi(t)$, and $|e(0)| < F_\phi(0)$.

According to (11) and (12), define a new funnel error variable $s_1(t)$ as

$$s_1(t)=\frac{e(t)}{F_\phi(t)-\|e(t)\|}, \tag{14}$$

where the funnel boundary $F_\phi(t)$ satisfies the condition given in (13). This variable will be employed to ensure the prescribed output performance.

The derivative of (14) is

$$\dot{s}_1=\frac{F_\phi\dot{e}-\dot{F}_\phi e}{(F_\phi-\|e\|)^2}=F_\phi\Phi_{\rm F}\dot{e}-\dot{F}_\phi\Phi_{\rm F}e, \tag{15}$$

where $\Phi_{\rm F}=\dfrac{1}{(F_\phi-\|e\|)^2}$ and

$$\begin{aligned}\ddot{s}_1=&F_\phi\Phi_{\rm F}\ddot{e}+F_\phi\dot{\Phi}_{\rm F}\dot{e}+\dot{F}_\phi\Phi_{\rm F}\dot{e}-\ddot{F}_\phi\Phi_{\rm F}e-\\&\dot{F}_\phi\dot{\Phi}_{\rm F}e-\dot{F}_\phi\Phi_{\rm F}\dot{e}=F_\phi\Phi_{\rm F}\ddot{e}+H_1,\end{aligned} \tag{16}$$

where

$$H_1=F_\phi\dot{\Phi}_{\rm F}\dot{e}+\dot{F}_\phi\Phi_{\rm F}\dot{e}-\ddot{F}_\phi\Phi_{\rm F}e-\dot{F}_\phi\dot{\Phi}_{\rm F}e-\dot{F}_\phi\Phi_{\rm F}\dot{e}.$$

3.2 Controller design

Considering (15) and (16), the sliding mode manifold is designed as

$$s_2=\dot{s}_1+\alpha s_1, \tag{17}$$

where $\alpha>0$. Differentiating s_2, we have

$$\dot{s}_2=\ddot{s}_1+\alpha\dot{s}_1. \tag{18}$$

Substituting (8) and (16) into (18) yields

$$\begin{aligned}&\dot{s}_2=F_\phi\Phi_{\rm F}\ddot{e}+H_1+\alpha\dot{s}_1=\\&F_\phi\Phi_{\rm F}(\dot{x}_2-\dddot{y}_{\rm d})+H_1+\alpha\dot{s}_1=\\&F_\phi\Phi_{\rm F}(h+bu-\dddot{y}_{\rm d})+H_1+\alpha\dot{s}_1=\\&F_\phi\Phi_{\rm F}(\kappa+bu-\dddot{y}_{\rm d})+\alpha\dot{s}_1,\end{aligned} \tag{19}$$

where the nonlinear function κ is

$$\kappa=h+\frac{H_1}{F_\phi\Phi_{\rm F}}.$$

Since κ is not easy to be exactly known, the model-based controllers cannot be applied directly. Hence, we adopt a neural network (9) to approximate the nonlinear function κ.

Assume that there exists a constant ideal weight matrix W^* so that the nonlinear function κ can be expressed as

$$\kappa=W^{*\rm T}\phi(\boldsymbol{X})+\varepsilon, \tag{20}$$

where the input vector $\boldsymbol{X}=[y_{\rm d}^{\rm T}\ \dot{y}_{\rm d}^{\rm T}\ \ddot{y}_{\rm d}^{\rm T}\ s_1^{\rm T}\ s_2^{\rm T}]^{\rm T}\in\mathbb{R}^5$.

In the following, a nonsingular terminal sliding mode neural funnel control approach is developed for tracking control of the motor servo system (8). To force s_2 converge to zero within a finite time, the nonsingular terminal sliding mode manifold is employed as

$$\beta|\dot{s}_2|^{q/p}\mathrm{sgn}\,s_2+s_2=0, \tag{21}$$

where $\beta>0$, p and q are positive odd integers with $p<q$.

Substituting (19) into (21) and using (20), the controller is designed as

$$\begin{cases}u=-u_0/b_0,\\ u_0=-\dddot{y}_{\rm d}+\hat{W}^{\rm T}\phi(\boldsymbol{X})+\mu\mathrm{sgn}\,s_2+\\ \qquad\dfrac{1}{F_\phi\Phi_{\rm F}}[\alpha\dot{s}_1+\dfrac{1}{\beta}|s_2|^{p/q}\mathrm{sgn}\,s_2],\end{cases} \tag{22}$$

where b_0 is the lower bound of b; p and q are positive odd integers with $p<q$; $\hat{W}$ is the estimate of the ideal weight W^* and μ is the upper bound of sum of the neural network approximation error ε and $\tilde{W}^{\rm T}\phi(\boldsymbol{X})$, where $\tilde{W}=W-\hat{W}$ is the weight estimation error of the neural network.

The adaptive law of $\hat{W}$ is given by

$$\dot{\hat{W}}=K\phi(\boldsymbol{X})s_2, \tag{23}$$

where K is a positive definite and diagonal matrix, and ν is a positive constant.

Substituting (22) into (19) yields

$$\begin{aligned}\dot{s}_2=&\ F_\phi\Phi_{\rm F}[\tilde{W}^{\rm T}\phi(\boldsymbol{X})+\varepsilon-\mu\mathrm{sgn}\,s_2]-\\&\frac{1}{\beta}|s_2|^{p/q}\mathrm{sgn}\,s_2.\end{aligned} \tag{24}$$

4 Stability analysis

In this section, a lemma and a theorem is provided to show the boundedness of all signals and the stability of the system (8) in both the reaching phase and the sliding phase, respectively.

Lemma 1 Assume that there exists a continuous positive definite function $V(t)$ satisfying the following inequality:

$$\dot{V}(t)+nV^\gamma(t)\leqslant 0,\ \ \forall t>t_0, \tag{25}$$

where $n>0$, $0<\gamma<1$ are constants. Then, for any given t_0, $V(t)$ satisfies the following inequality:

$$V^{1-\gamma}(t)\leqslant V^{1-\gamma}(t_0)-n(1-\gamma)(t-t_0),\ \ t_0\leqslant t\leqslant t_{\rm s},$$

and

$$V(t)\equiv 0,\ \ \forall t\geqslant t_{\rm s}$$

with $t_{\rm s}$ given by

$$t_{\rm s}\leqslant t_0+\frac{V^{1-\gamma}(t_0)}{n(1-\gamma)}.$$

Theorem 1 Consider the motor servo system (8) with unknown nonlinear saturation (2), nonsingular terminal sliding manifold (21), control law (22), and weight update law (23), then

1) All signals of the closed-loop system are bounded.

2) The nonsingular terminal sliding manifold s_2 can converge to zero in finite time by using controllers (22), if the design parameter $\mu>\varepsilon_N+\|\tilde{W}^{\rm T}\phi(\boldsymbol{X})\|_{\rm F}$.

3) The tracking error e will fall into proscribed boundaries.

Proof 1) Choose the following Lyapunov function candidate

$$V = \frac{1}{2k_{\rm m}}s_2^2 + \frac{1}{2}\tilde{W}^{\rm T}K\tilde{W}, \tag{26}$$

where $k_{\rm m} = F_{\phi}\Phi_{\rm F} > 0$.

Differentiating (26) with respect to time and using (24), we have

$$\begin{aligned}\dot{V} = &\frac{1}{k_{\rm m}}s_2\dot{s}_2 - \tilde{W}^{\rm T}K\dot{\hat{W}} = \\ &s_2[\tilde{W}^{\rm T}\phi(\boldsymbol{X}) + \varepsilon - \mu{\rm sgn}\, s_2 - \\ &F_{\phi}\Phi_{\rm F}\frac{1}{\beta}|s_2|^{p/q}{\rm sgn}\, s_2)] - \tilde{W}^{\rm T}K^{\rm T}\dot{\hat{W}} = \\ &\tilde{W}^{\rm T}[s_2\phi(\boldsymbol{X}) - K^{\rm T}\dot{\hat{W}}] + \varepsilon s_2 - \mu|s_2| - \\ &F_{\phi}\Phi_{\rm F}\frac{1}{\beta}|s_2|^{(p+q)/q}{\rm sgn}\, s_2.\end{aligned} \tag{27}$$

Substituting (23) into (27) yields

$$\dot{V} \leqslant -F_{\phi}\Phi_{\rm F}\frac{1}{\beta}|s_2|^{(p+q)/q} \leqslant 0. \tag{28}$$

Inequality (27) implies that both s_2 and $\tilde{W}$ are bounded. Meanwhile, considering (17) and the boundedness of W^*, we can conclude s_1, $\dot{s_1}$, and $\hat{W}$ are bounded, and thus from (22) and (14), we can obtain u, e and $\dot{e}$ are all bounded. Furthermore, the boundedness of $y_{\rm d}$, $\dot{y}_{\rm d}$ and $\ddot{y}_{\rm d}$ can lead to the boundedness of s_2 according to (17). As a result, and $\dot{s}_2$ is bounded due to the boundedness of g_{u_ξ}. Therefore, all signals of the closed loop system are bounded.

From (26)–(28), the stability of the system (8) with control laws (22) and weight update law (23) has been proved. However, it is not necessary for the terminal sliding manifold s_2 to converge to zero in finite time. Therefore, further proof should be given to guarantee that the terminal sliding manifold s_2 converge to zero in finite time.

2) From (29), we can see that the sigmoid function $\phi(\boldsymbol{X})$ is bounded by $0 < \phi_i(\boldsymbol{X}) < n_0$, $i = 1, \cdots, n_1$, with $n_0 = \max\{|\frac{a}{b} + d|, |\frac{a}{b+1} + d|\}$. Therefore, $\phi(\boldsymbol{X})$ is bounded by

$$\|\phi(\boldsymbol{X})\| \leqslant n_0\sqrt{n_1},$$

where $\|\cdot\|$ denotes the Euclidean norm of a vector, $\phi(\boldsymbol{X}) = [\phi_1(\boldsymbol{X})\ \ \phi_2(\boldsymbol{X})\ \ \cdots\ \ \phi_{n_1}(\boldsymbol{X})]^{\rm T}$.

From the property of Forensics norm, it can be obtained that

$$\|\tilde{W}^{\rm T}\phi(\boldsymbol{X})\|_{\rm F} \leqslant \|\tilde{W}\|_{\rm F}\|\phi(\boldsymbol{X})\|.$$

Select another Lyapunov function candidate

$$V_1 = \frac{1}{2k_{\rm m}}s_2^2. \tag{29}$$

Differentiating (29) with respect to time and using (24), we have

$$\begin{aligned}\dot{V}_1 = &\frac{1}{k_{\rm m}}s_2\dot{s}_2 = \\ &s_2[\tilde{W}^{\rm T}\phi(\boldsymbol{X}) + \varepsilon - \mu{\rm sgn}\, s_2 - \\ &F_{\phi}\Phi_{\rm F}\frac{1}{\beta}|s_2|^{p/q}{\rm sgn}\, s_2)].\end{aligned} \tag{30}$$

Since $\mu > \varepsilon_N + \|\tilde{W}^{\rm T}\phi(\boldsymbol{X})\|_{\rm F}$, (30) can be rewritten as

$$\begin{aligned}\dot{V}_1 \leqslant &-F_{\phi}\Phi_{\rm F}\frac{1}{\beta}|s_2|^{(p+q)/q} = \\ &-k_1 2^{(p+q)/2q}V^{(p+q)/2q} = \\ &-k_2 V_1^{k_3}.\end{aligned} \tag{31}$$

Then, we can obtain

$$\dot{V}_1 + k_2 V_1^{k_3} \leqslant 0. \tag{32}$$

According to Lemma 1, it can be concluded that the fast terminal sliding manifold s_2 can converge to the equilibrium point within a finite time t_1 given by

$$t_1 = \frac{V^{1-k_3}(t_0)}{k_2(1-k_3)}. \tag{33}$$

3) Once the sliding surface $s_2 = 0$ is achieved. the states of system (8) will remain on it and the system has the invariant properties. On the sliding surface $s_2 = 0$, we can obtain

$$\dot{s}_1 = -\alpha s_1. \tag{34}$$

Constructing the following Lyapunov candidate

$$V_2 = \frac{1}{2}s_1^2, \tag{35}$$

and differentiating V_2 along (34), we have

$$\dot{V}_2 = -\alpha s_1^2 \leqslant 0. \tag{36}$$

Then, we can conclude that the funnel error s_2 will converge to the equilibrium point. Thus, from (14), the tracking error e will fall into the prescribed boundaries.

Remark 2 Since the discontinuous switching function ${\rm sgn}(\cdot)$ shown in (22) may result in the chattering phenomenon, the following continuous $\Delta(s)$ is employed instead in the simulation section:

$$\Delta(s) = \begin{cases}{\rm sgn}\, s, & |\dfrac{s}{\zeta}| \geqslant 1, \\ \dfrac{|s|}{|s| + \zeta}{\rm sgn}\, s, & |\dfrac{s}{\zeta}| < 1,\end{cases} \tag{37}$$

where ζ is a positive constant defining the thickness of the boundary layer.

When $|s| \geqslant \zeta$, the proof can be easily accomplished according to the proof of Theorem 1. When $|s| < \zeta$, following the proof steps in [30], we can also obtain

$$\dot{V} \leqslant -F_{\phi}\Phi_{\rm F}\frac{1}{\beta}|s_2|^{(p+q)/q} \leqslant 0,$$

and

$$\dot{V}_1 \leqslant -F_\phi \Phi_{\rm F} \frac{1}{\beta}|s_2|^{(p+q)/q} = -k_1 2^{(p+q)/2q} V^{(p+q)/2q}.$$

Actually, there exists a small positive constant ϵ such that $\epsilon \leqslant (|s| + \zeta)$. With this modified controller, the chattering can be eliminated and the finite-time convergence is guaranteed in the whole tracking process.

5 Simulation results

In this section, the following three other control approaches are presented for the performance comparison with the proposed NTSMFC scheme.

1) PID control

$$u = k_{\rm p} e + k_{\rm i} \int e{\rm d}t + k_{\rm d}\dot{e}, \tag{38}$$

where $k_{\rm p} = 20$, $k_{\rm i} = 0.05$, and $k_{\rm d} = 4$.

2) Neural-network sliding mode control (SMC)[31]

$$\begin{cases} u = -\dfrac{u_0}{b_0}, \\ u_0 = -\ddot{y}_{\rm d} + \hat{W}^{\rm T}\phi(\boldsymbol{X}) + \mu{\rm sgn}\, s_2 + \alpha\dot{s}_1 + k_1 s_2, \end{cases} \tag{39}$$

where $s_1 = e$, $b_0 = 6$, $\alpha = 2$, $k_1 = 10$, and $\mu = 0.1$.

3) Neural-network sliding mode control (NTSMC)[21]

$$\begin{cases} u = -\dfrac{u_0}{b_0}, \\ u_0 = -\ddot{y}_{\rm d} + \hat{W}^{\rm T}\phi(\boldsymbol{X}) + \mu{\rm sgn}\, s_2 + \\ \qquad \alpha\dot{s}_1 + \dfrac{1}{\beta}|s_2|^{p/q}{\rm sgn}\, s_2, \end{cases} \tag{40}$$

where $s_1 = e$, $\alpha = 2$, $\beta = 0.2$, $k_1 = 10$, $p = 5$, $q = 7$, $b_0 = 6$ and $\mu = 0.1$.

For fair comparison, all control parameters are fixed for various reference signals. The initial states of the system are $x_1(0) = 0$, $x_2(0) = 0$. The NN parameters are $K = 0.1$, $a = 2$, $b = 10$, $c = 1$, $d = -10$. The parameters of funnel boundary (13) are chosen as $\delta_0 = 100$, $\delta_\infty = 0.3$ and $a_0 = 3$. And the control law (22), where $\alpha = 2$, $\beta = 0.2$, $k_1 = 10$, $p = 5$, $q = 7$, $b_0 = 6$ and $\mu = 0.1$. The system is select as $h = 0.2x_2 \sin x_2$ and $b = 6$. The saturation bound $v_{\max} = 1$.

In the following, three different cases are performed to compare four different controllers.

Case 1 Sinusoidal wave. $y_{\rm d} = 0.5\sin t$ is employed as the reference. Simulation has been conducted, and two comparative results are shown in Fig.3. The tracking performance and tracking errors are depicted in Fig.3(a) and Fig.3(b), respectively. As shown in Fig.3(a), when tracking the sinusoidal wave, the NTSMFC and the NTSMC have the comparatively lower overshoot, while the PID control scheme has the largest overshoot. From Fig.3(b), we can see that the NTSMFC has the smallest tracking error and fastest convergence speed; NTSMC has the largest overshoot at the beginning, and the PID scheme has the largest steady tracking error.

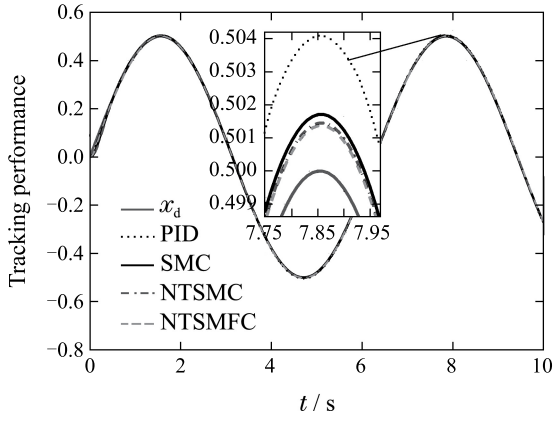

(a)

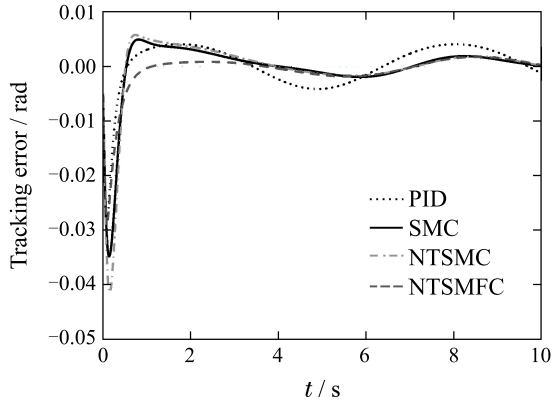

(b)

Fig. 3 Tracking performance of $0.5\sin t$

Case 2 Sinusoidal wave with harmonic. The tracking performance of the reference signal $0.5(\sin t + \sin 0.5t)$ is shown in Fig.4. Among the four schemes, the NTSMFC has the smallest overshoot and tracking error with the fastest convergence speed. The SMC and NTSMC have a large overshoot at the beginning, and PID control has largest tracking error when time goes to the infinity. Obviously, NTSMFC has the best performance when tracking the the reference signal $0.5(\sin t + \sin 0.5t)$.

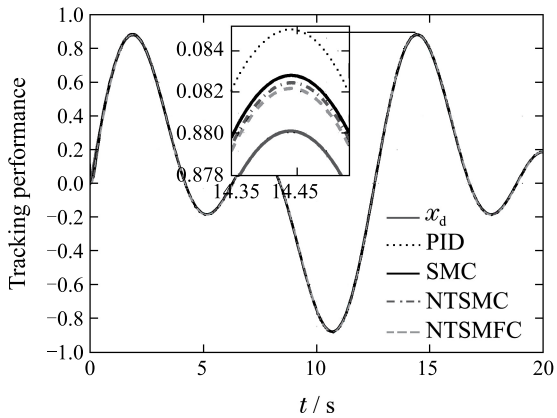

(a)

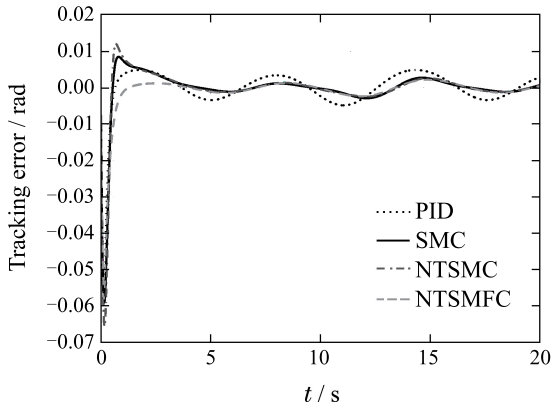

(b)

Fig. 4 Tracking performance of $0.5(\sin t + \sin 0.5t)$

Case 3 Step signal. To further justify the transient performance (e.g., overshoot), a step signal with amplitude 1 rad is employed. Control parameters are set the same as those given before. As shown in Fig.5, we can see that PID control has comparatively larger overshoot. Besides, the proposed scheme can converge within 1 s, while PID control costs 1.5 s; SMC and NTSMC cost more than 4 s to achieve the same performance. Therefore, we can conclude that the proposed NTSMFC has the best transient performance.

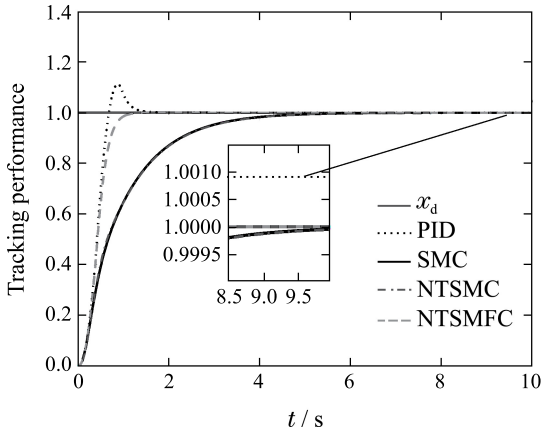

Fig. 5 Tracking performance of step signal

In order to show the comparison performance more convincingly, several indices are provided to evaluate the performance of the four controllers.

1) IAE $= \int_0^{t_\mathrm{f}} |e(t)|\mathrm{d}t$, which is the integrated absolute value of the error to measure intermediate tracking result.

2) ITAE $= \int_0^{t_\mathrm{f}} t|e(t)|\mathrm{d}t$, which is the integral of the time multiplied by the absolute value of the error, and used to measure the tracking performance with time behaving as a factor to emphasize errors occurring late.

3) ISDE $= \int_0^{t_\mathrm{f}} (e(t) - e_0)^2\mathrm{d}t$, which is the integrated square error and used to demonstrate the smoothness of the profile.

The simulation results in terms of performance indices are provided by Tables 1–3. From Tables 1–2, we can see that when tracking sinusoidal waves, the proposed NTSMFC scheme has the smallest IAE, ITAE and ISDE, which means it performs best among four controllers. From Table 3, it can be concluded that when tracking the step signal, although PID controller has the smallest ISDE, it has the larger ITAE and IAE than NTSMFC, while SMC and NTSMC have relatively large IAE, ITAE and ISDE.

Therefore, all the aforementioned simulation results clearly show that the proposed NTSMFC scheme can achieve the best tracking performance with respect to tracking errors and convergence speed.

Table 1 Comparison for tracking sinusoidal wave $y_\mathrm{d} = 0.5\sin t$

Controller	IAE/rad	ITAE/ (rad · s^{-1})	ISDE/rad^2
PID	0.0287	0.1267	0.0087
SMC	0.0257	0.0653	0.0070
NTSMC	0.0295	0.0696	0.0092
NTSMFC	0.0178	0.0569	0.0036

Table 2 Comparison for tracking sinusoidal wave $y_\mathrm{d} = 0.5(\sin t + \sin 0.5t)$

Controller	IAE/rad	ITAE/ (rad · s^{-1})	ISDE/rad^2
PID	0.0667	0.5141	0.0890
SMC	0.0485	0.2391	0.0483
NTSMC	0.0525	0.2460	0.0567
NTSMFC	0.0398	0.2230	0.0340

Table 3 Comparison for tracking step signal $y_\mathrm{d} = 1$

Controller	IAE/rad	ITAE/ (rad · s^{-1})	ISDE/rad^2
PID	0.4510	0.1765	2.0323
SMC	0.9999	0.9699	12.5248
NTSMC	0.9999	0.9749	12.5231
NTSMFC	0.4459	0.1261	2.7131

6 Conclusions

In this paper, a nonsingular terminal sliding mode funnel control (NTSMFC) scheme is proposed to achieve a prescribed tracking performance for motor servo systems with unknown input saturation. The non-smooth saturation is transformed into an affine form by defining a smooth non-affine function and using the mean-value theorem. A new constraint variable is employed and the tracking error will be forced to fall into prescribe boundaries. By using a simple sigmoid neural network to approximate the unknown system nonlinearity, a nonsingular terminal sliding mode funnel control is developed for the prescribed tracking performance of the motor servo system. With the proposed scheme, no prior knowledge is required on the input saturation bound, and the convergence of the position tracking error is guaranteed via the Lyapunov synthesis. Our further work is to apply the proposed scheme to a practical motor servo system.

References:

[1] LI S H, LIU Z. Adaptive speed control for permanent-magnet synchronous motor system with variations of load inertia [J]. *IEEE Transactions on Industrial Electronics*, 2009, 56(8): 3050 – 3059.

[2] MORAWIEC M. The adaptive backstepping control of permanent magnet synchronous motor supplied by current source inverter [J]. *IEEE Transactions on Industrial Informatics*, 2013, 9(2): 1047 – 1055.

[3] LIU G, CHEN L, ZHAO W, et al. Internal model control of permanent magnet synchronous motor using support vector machine generalized inverse [J]. *IEEE Transactions on Industrial Informatics*, 2013, 9(2): 890 – 898.

[4] TEE K P, REN B B, GE S S. Control of nonlinear systems with time-varying output constraints [J]. *Automatica*, 2011, 47(11): 2511 – 2516.

[5] NIU B, ZHAO J. Barrier Lyapunov functions for the output tracking control of constrained nonlinear switched systems [J]. *Systems & Control Letters*, 2013, 62(10): 963 – 971.

[6] LI Y, LI T, JING X. Indirect adaptive fuzzy control for input and output constrained nonlinear systems using a barrier Lyapunov function [J]. *International Journal of Adaptive Control and Signal Processing*, 2014, 28(2): 184 – 199.

[7] BECHLIOULIS C P, ROVITHAKIS G A. Robust partial-state feedback prescribed performance control of cascade systems with unknown nonlinearities [J]. *IEEE Transactions on Automatic Control*, 2011, 56(9): 2224 – 2230.

[8] NA J. Adaptive prescribed performance control of nonlinear systems with unknown dead zone [J]. *International Journal of Adaptive Control and Signal Processing*, 2013, 27(5): 426 – 446.

[9] NA J, CHEN Q, REN X M, et al. Adaptive prescribed performance motion control of servo mechanisms with friction compensation [J]. *IEEE Transactions on Industrial Electronics*, 2014, 61(1): 486 – 494.

[10] ILCHMAN A, SCHUSTER H. Tracking control with prescribed transient behavior degree [J]. *Systems & Control Letters*, 2006, 55(5): 396 – 406.

[11] ILCHMAN A, RYAN E P, TRENN S. PI-funnel control for two mass systems [J]. *IEEE Transactions on Affective Computing*, 2009, 54(4): 918 – 923.

[12] HACKL C M, ENDISCH C, SCHRODER D. Contribution to non-identifier based adaptive control in mechatronics [J]. *Robotics and Autonomous Systems*, 2009, 57(10): 996 – 1005.

[13] HACKL C M. High-gain position control [J]. *International Journal of Control*, 2011, 84(10): 1695 – 1716.

[14] HAN S I, LEE J M. Recurrent fuzzy neural network backstepping control for the prescribed output tracking performance of nonlinear dynamic systems [J]. *ISA transactions*, 2014, 53(1): 33 – 43.

[15] HAN S I, LEE J M. Fuzzy echo state neural networks and funnel dynamic surface control for prescribed performance of a nonlinear dynamic system [J]. *IEEE Transactions on Industrial Electronics*, 2014, 61(2): 1099 – 1112.

[16] IMURA J, SUGIE T, YOSHIKAWA T. Adaptive robust control of robot manipulators-Theory and experiment [J]. *IEEE Transactions on Robotics and Automation*, 1994, 10(5): 705 – 710.

[17] XU L, YAO B. Adaptive robust precision motion control of linear motors with negligible electrical dynamics: theory and experiments [J]. *IEEE Transactions on Mechatronics*, 2001, 6(4): 444 – 452.

[18] MAN Z H, YU X H. Adaptive terminal sliding mode tracking control for rigid robotic manipulators with uncertain dynamics [J]. *International Journal of Mechanical Systems, Machine Elements, and Manufacturing*, 1997, 40(3): 493 – 502.

[19] FENG Y, YU X H, MAN Z H. Non-singular terminal slidng mode control of rigid manipulators [J]. *Automatica*, 2002, 38(12): 2159 – 2167.

[20] YU S, YU X H, SHIRINZADEHC B. Continuous finite-time control for robotic manipulators with terminal sliding mode [J]. *Automatica*, 2005, 41(11): 1957 – 1964.

[21] CHEN S Y, LIN F J. Robust nonsingular terminal sliding-mode control for nonlinear magnetic bearing system [J]. *IEEE Transactions on Control Systems Technology*, 2011, 19(3): 636 – 643.

[22] PEREZ-ARANCIBIA N O, TSAO T C, GIBSON J S. Saturation-induced instability and its avoidance in adaptive control of hard disk drives [J]. *IEEE Transactions on Control Systems Technology*, 2010, 18(2): 368 – 382.

[23] GAO W Z, SELMIC R R. Neural network control of a class of nonlinear systems with actuator saturation [J]. *IEEE Transactions on Neural Networks*, 2006, 17(1): 147 – 156.

[24] HU Q L, MA G F, XIE L H. Robust and adaptive variable structure output feedback control of uncertain systems with input nonlinearity [J]. *Automatica*, 2008, 44(4): 552 – 559.

[25] CHEN M, GE S S, HOW B. Robust adaptive neural network control for a class of uncertain MIMO nonlinear systems with input nonlinearities [J]. *IEEE Transactions on Neural Networks*, 2010, 21(5): 796 – 812.

[26] CHEN M, GE S S, REN B B. Adaptive tracking control of uncertain MIMO nonlinear systems with input constraints [J]. *Automatica* 2011, 47(3): 452 – 455.

[27] ZHANG X, WANG M, ZHAO J. Stability analysis and antiwindup design of uncertain discrete-time switched linear systems subject to actuator saturation [J]. *Journal of Control Theory and Applications*, 2012, 10(3): 325 – 331.

[28] WEN C Y, ZHOU J, LIU Z T, et al. Robust adaptive control of uncertain nonlinear systems in the presence of input saturation and external disturbance [J]. *IEEE Transactions on Automatic Control*, 2011, 56(7): 1672 – 1678.

[29] WANG H, CHEN B, LIU X, et al. Adaptive neural tracking control for stochastic nonlinear strict-feedback systems with unknown input saturation [J]. *Information Sciences*, 2014, 269(6): 300 – 315.

[30] LIU H T, ZHANG T. Neural network-based robust finite-time control for robotic manipulators considering actuator dynamics [J]. *Robotics and Computer-Integrated Manufacturing*, 2013, 29(2): 301 – 308.

[31] CHEN Q, NAN Y R, JIN Y. Neural sliding mode control for turntable servo system with unknown deadzone [C] // *Proceedings of the 32nd Chinese Control Conference*. Xi'an, China, 2013.

作者简介:

陈 强 (1984–), 男, 讲师, 目前研究方向为交流伺服电机控制、非线性摩擦和死区补偿、自适应神经网络控制等, E-mail: sdnjchq@zjut.edu.cn;

汤筱晴 (1993−), 女, 目前研究方向为滑模自适应控制, E-mail: shinotang222@gmail.com.